Chapter 17

Quantitative Evaluation of Plant Actin Cytoskeletal Organization During Immune Signaling

Yi-Ju Lu and Brad Day

Abstract

High spatial and temporal resolution microscopy-based methods are valuable tools for the precise real-time imaging of changes in cellular organization in response to stimulus perception. Here, we describe a quantitative method for the evaluation of the plant actin cytoskeleton during immune stimulus perception and the activation of defense signaling. As a measure of the biotic stress-induced changes in actin filament organization, we present methods for analyzing changes in actin filament organization following elicitation of pattern-triggered immunity and effector-triggered immunity. Using these methods, it is possible to not only quantitatively evaluate changes in actin cytoskeletal organization following biotic stress perception, but to also use these protocols to assess changes in actin filament organization following perception of a wide range of stimuli, including abiotic and developmental cues. As described herein, we present an example application of this method, designed to evaluate changes in actin cytoskeletal organization following pathogen perception and immune signaling.

Key words Actin cytoskeleton, Confocal microscopy, Quantitative evaluation, ETI, PTI, *Pseudomonas syringae*, Immune signaling, PAMP

1 Introduction

The actin cytoskeleton is required for the function of numerous cellular processes, including those required for growth, development, response to the environment, and immunity [1]. For example, in plants, abiotic stress, as well as a multitude of pathogen-derived elicitors, has been demonstrated to induce rapid and transient changes in actin organization, including polymerization and bundling [2–6]. However, our understanding of the role of actin, including the purpose of the incessant remodeling to the host cytoskeleton during stress signaling, is largely corollary and lacking a mechanistic definition of the role of actin as a required component of the signaling cascade. In plants, a multitude of immune-eliciting bacterial strains and purified pathogen elicitors cause rapid and transient increases in actin polymerization [2]. These changes have been demonstrated to be specific, and only occur when the

plant has its full complement of corresponding pattern recognition receptors and known components of the pattern receptor complex. To fully define the role of the plant actin cytoskeleton, including the ability to rapidly and accurately associate changes in cytoskeletal organization with the precise activation of specific signaling cascades, requires a comprehensive, and parallel, analysis of the genetic, biochemical, and cellular processes during stimulus perception. In recent years, this approach has been successfully employed to define the plant cell response, including the activation of immunity, in response to pathogen perception.

Recent advances in live cell imaging technologies have made it possible to define the temporal and spatial changes in cytoskeletal organization, and to accurately associate these changes with concomitant changes in host physiology and cell signaling [2, 7–9]. Of these advanced technologies, fluorescent imaging of the cytoskeleton has emerged as one of the most reliable tools for monitoring changes in the microtubule and actin filament array [10]. In this Chapter, we describe confocal microscopy-based methods for imaging of the plant actin cytoskeleton, including quantification of changes in filament organization, during host infection with phytopathogenic microbes. As a highly robust method to define and associate changes in actin filament organization with concomitant changes in the host cell physiology during pathogen infection, the procedure presented herein is a reliable, highly quantitative method to visualize and describe changes in host cell organization during stress response and signaling.

2   Materials

All liquid reagents described herein should be prepared using ultrapure, sterile deionized water (dH$_2$O). Freshly prepared solutions should be stored at room temperature, unless otherwise indicated.

2.1   General Reagents and Disposables

1. Polystyrene sterile six-well flat bottom plates.
2. Sterile 100 × 100 mm Petri dishes.
3. Fine-tip forceps.
4. Incubator, 28 °C.

2.2   Bacterial Culture and Media Preparation

1. NYGA (nutrient yeast glucose agar; [11]) media: 0.5% Bacto peptone, 0.3% yeast extract, 2% (v/v) glycerol, 15% Bacto agar. Autoclave media at 121 °C for 45 min. Cool NYGA media to 55 °C, and then add antibiotics, if necessary, mix, and pour 25 mL of media into 100 × 100 mm petri dishes. Cool to room temperature.

2. Antibiotic stock concentrations: rifampicin (100 mg/mL) and kanamycin (50 mg/mL). Antibiotic working concentrations: rifampicin (100 μg/mL) and kanamycin (25 μg/mL). Antibiotic stock solutions should be stored at −20 °C.

2.3 Arabidopsis Thaliana Growth and Treatment

The methods described herein have been optimized for the visualization of Arabidopsis epidermal cells following treatment with purified pathogen elicitors and/or dip-inoculation with *Pseudomonas syringae* pv. *tomato* DC3000 (*Pst* DC3000). Based on the sum of our experiences, the methods described below are suitable for the evaluation of any number of plant pathogenic bacteria, including those harboring heterologously expressed type three effectors (T3Es).

1. Arabidopsis plants expressing GFP-fABD2 [12].
2. Fiberglass window screen (Fig. 1a).
3. Potting soil mix (*see* **Note 1**).
4. Rubber bands.
5. Growth chamber conditions: 20 °C, 16 h light–8 h dark cycle with 60% relative humidity and a light intensity of 120 μmol photons/m²s.
6. Resuspension solution: 10 mM $MgCl_2$.
7. Dip inoculation solution: 10 mM $MgCl_2$ + 0.02% Silwet.
8. Spectrophotometer.
9. Conical Falcon tubes, 15 mL.

2.4 Pathogen Elicitors

In the case presented herein, we broadly refer to pathogen elicitors as pathogen-associated molecular patterns (PAMPs; e.g., flg22, chitin, elf18; [13]). Peptide elicitors can be synthesized and purchased from a number of companies, and should be synthesized at >99% purity (*see* **Note 2**). For the generation of the PAMP chitin, refer to the methods presented in Kaku et al. [14]. Stock solutions of purified pathogen elicitors should be prepared in sterile dH_2O and stored at −20 °C.

The amino acid sequences of two commonly used *Pst* DC3000 PAMPs are as follows:

1. Flg22 peptide: Q-R-L-S-T-G-S-R-I-N-S-A-K-D-D-A-A-G-L-Q-I-A [15].
2. Elf18 peptide: ac-S-K-E-K-F-E-R-T-K-P-H-V-N-V-G-T-I-G [16].

2.5 Preparing Samples for Laser Scanning Confocal Microscopy

1. Confocal microscope with 60× objective.
2. Glass slides (Pre-cleaned, 1″ × 3″, 1.2 mm).
3. Cover slides: 18 × 18 mm, 1.5 oz.
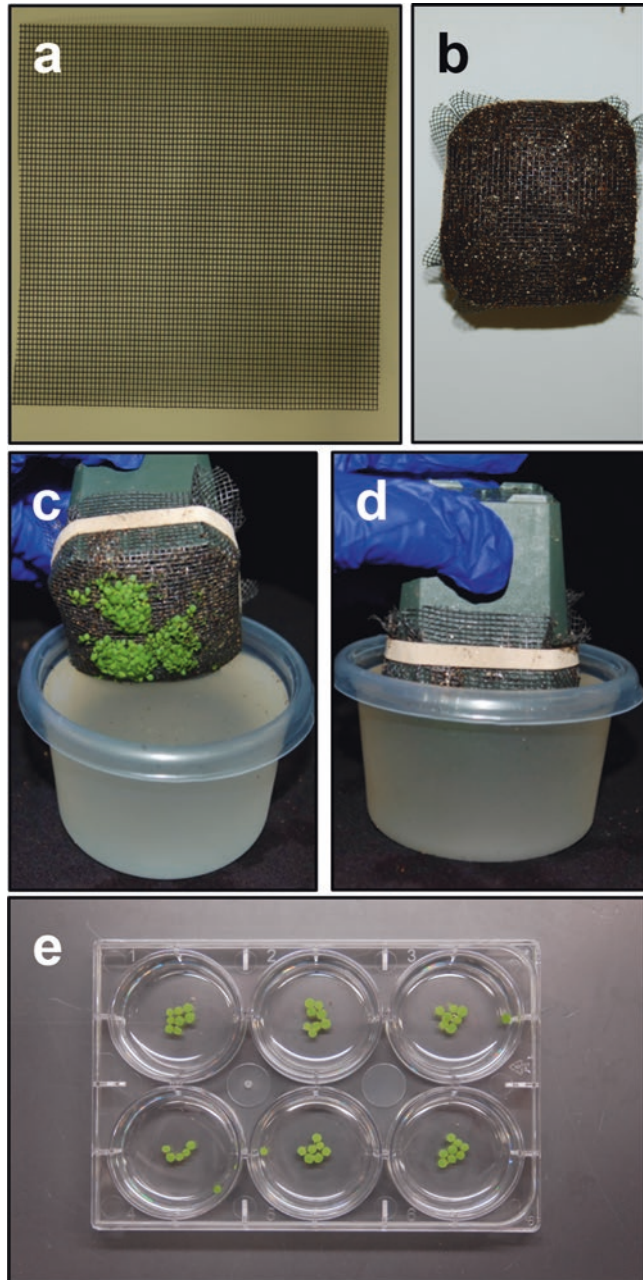
Fig. 1 Treatment of Arabidopsis seedlings with pathogen and pathogen elicitors for induction of immunity and elicitation of changes in host actin cytoskeletal organization. (**a**) Fiberglass insect screen. (**b**) 10–12-day-old seedling in pots covered with fiberglass insect screen. (**c**, **d**) 10–12-day-old Arabidopsis are dip-inoculated in a suspension of *Pseudomonas syringae.* (**e**) Pathogen elicitor treatment of detached Arabidopsis cotyledons

2.6 Image Analysis Software

1. Standard confocal microscopy image collection and analysis software.

2. Fiji image analysis software package (formerly called ImageJ). Free download at: http://fiji.sc/Fiji.

3. The scripts (.txt files) for actin skewness and density analysis, first published by [8], can be downloaded at:

   Skewness:
   http://www.daylab.plp.msu.edu/wp-content/uploads/2015/10/Skewness.txt.
   Density:
   http://www.daylab.plp.msu.edu/wp-content/uploads/2015/10/Density.txt.

3   Methods

All plant inoculation procedures and microscopy analyses should be performed at room temperature (ca. 25 °C).

3.1 Plant Growth

1. Sow GFP-fABD2-expressing Arabidopsis seeds in pots filled with soil and fitted with fiberglass screen (Fig. 1b; *see* **Note 3**). Seeds should be sewn evenly across the pot; after seed germination, plants can be thinned, if necessary, using fine-tip forceps.

2. Stratify seeds at 4 °C in the dark for 3 days.

3. After stratification, transfer pots to an environmentally controlled growth chamber, and water plants as necessary.

4. For actin cytoskeleton imaging during immune elicitation, 10–12-day-old Arabidopsis seedlings are used (Fig. 1c).

3.2 Bacteria Growth and Plant Inoculation

1. Remove bacteria from the −80 °C and streak onto NYGA plates containing appropriate antibiotics, if required, and grow *Pst* DC3000 strains for 2 days at 28 °C.

2. After 2 days growth, re-streak *Pst* DC3000 strains onto fresh NYGA plates containing antibiotics and incubate an additional 16–20 h at 28 °C.

3. After 16–20 h of additional growth, pipette 5 mL of $MgCl_2$ buffer on NYGA plates containing bacterial (i.e., *Pst* DC3000).

4. Gently scrape bacteria from the plate and collect the $MgCl_2$-*Pst* DC3000 solution, transferring into a fresh (sterile) 15 mL Falcon tube.

5. To determine the concentration of the bacterial solution, transfer 100 μL of the bacterial suspension into an Eppendorf tube containing 900 μL $MgCl_2$ buffer (i.e., a 1:10 dilution of your stock solution).

6. Determine concentration of bacteria by measuring the optical density (OD) of the suspension at 600_{nm} using a standard laboratory spectrophotometer.

7. Adjust the concentration of the bacterial suspension to 3×10^7 colony-forming units/mL (CFU/mL) in the required volume of dip inoculation buffer. $OD_{600nm} = 1.0 = 1 \times 10^8$ CFU/mL.

8. For plant inoculation, for example, prepare 200 mL of the bacterial suspension. This is an amount sufficient to dip-inoculate three pots of 10- to 12-day-old seedlings.

9. Invert pots containing Arabidopsis seedlings into the bacterial solution, submerging for 30 s. Gently swirl pots to ensure uniform treatment of the seedlings (Fig. 1c, d)

10. After inoculation, return pots to plant growth trays and place a clear plastic dome lid on flats for 1 h to maintain high relative humidity. After 1 h, remove the dome and return flats to the growth chamber.

11. Periodically observe inoculated seedlings over the course of the experiment. This is most important beginning at around 24–28 h post inoculation (hpi) to ensure that tissue collapse is not occurring.

12. For evaluation of actin cytoskeletal changes during ETI, image seedlings at 24–28 hpi (*see* **Note 4**).

3.3 Inoculation with PAMP Elicitors (PTI)

1. Peptide elicitors, from −20 °C stock solutions, are dissolved in 10 mL of 10 mM $MgCl_2$ to yield working stock solutions. The final working concentration of each elicitor (flg22, elf26, and chitin) ranges from 1 to 25 μM; for our experiments, we typically use a final concentration of 10 μM. For other elicitors, the concentration may vary, depending on the previously defined bioactive concentration.

2. Pipette 5 mL of the elicitor solution into a sterile six-well flat bottom plate.

3. The cotyledons from 10- to 12-day-old Arabidopsis seedling are then floated in the elicitor solution contained in the six-well plate. Approximately 10–15 cotyledons can be placed in each well containing the elicitor solution (Fig. 1e).

4. Return the cover (to maintain humidity), and store plates under ambient light at room temperature. *The incubation time may vary, depending on the elicitor.* For the above noted PAMPs (i.e., flg22, elf26, chitin), incubate over a short time course of 0, 0.5, 1, 2, 4, and 6 h, imaging at each time point. In most cases, optimal time for imaging is approximately 1–2 hpi [2].

3.4 Laser Scanning Confocal Microscopy: Image Collection

1. Images are collected using a laser confocal scanning microscope equipped with a 60× objective. Sample excitation at 488 nm (GFP), emission detection at 495–525 nm. For image

acquisition, 2× magnification is used at a resolution of 800 × 800 pixels.

2. Collect 4–5 images of the lower epidermal pavement cells from one cotyledon (*see* **Note 5**).

3. For each image, collect 25 serial stacks, with an interval of 0.5 μm from the plasma membrane (Fig. 2; *see* **Notes 6** and **7**).

4. Save the original image files for skewness and density analyses, described below. For skewness analysis, collect maximum projections of 25 serial stacks each image in the stack as a TIFF file format for skewness analysis.

3.5 **Image Analysis**	Recent studies have described the imaging and quantification of changes in actin filament organization using two key parameters: Skewness and Density [2, 8]. In short, Skewness is an indirect measure of the degree of actin filament bundling, while Density, also referred to as 'Percent Occupancy', indicates the relative abundance of actin filament signal within the cell.
3.5.1 Skewness Analysis	1. Perform Skewness analysis using the Fiji software package. The source files for Skewness analysis are the merged image files, representing 25 stacks, collected as described above. As noted above, these files should be in TIFF format.

2. Open the Fiji software package.

3. From the Fiji 'Menu', select **File ► Import ► Image Sequence**, and select the folder that contains the TIFF image files to be analyzed.

4. In the **Sequence Options** check the box to select '**Convert to 8-bit Grayscale'** and '**Sort names numerically**'. All of the remaining options should be left at the default settings. Click '**OK**'.

5. A new image stack, containing all images (i.e., 25 images, as noted in '**step 4**', above) will appear (Fig. 2).

6. From the Fiji 'Menu' bar, select **Image ► Adjust ► Threshold**. In the Threshold window, check '**Dark Background**'. Click '**Set**'. In the '**Set Threshold Levels**' window, set the '**Lower Threshold Level**' to **20**, and the '**Upper Threshold Level**' to **255**. Click '**OK**'. Leave the '**Threshold**' window open, and click on image window.

7. From the Fiji 'Menu' bar, select **Plugin ► Macros ► Install ► Skewness script**. At this step, locate the Skewness script (.txt file), downloaded as described above, and select '**Open**'.

8. From the Fiji '**Menu**', select **Plugin ► Macros ► Skewness**. |

At this point, the processing script will being running, and the output of this will yield skewness values for each image, presented in a separate, 'Results', window.
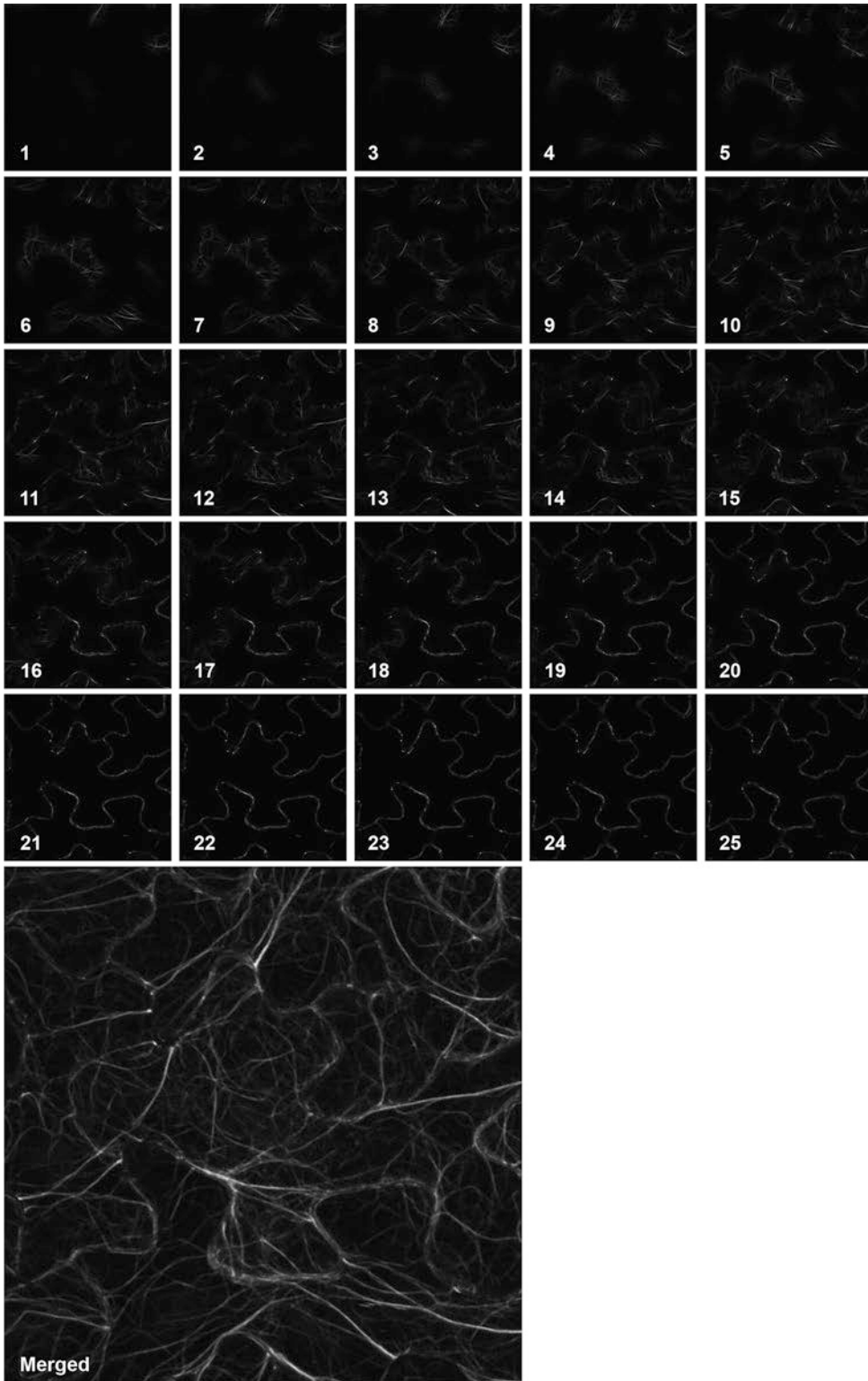
Fig. 2 Twenty-five Z-series image stacks collected using confocal laser scanning microscopy. The image stacks are collected in 0.5 μm intervals. The projection, which is the sum of the merged image stacks, is shown at the bottom left

9. Highlight and copy the output (i.e., '**sigNum**' and '**skewness**') and paste into a new Excel file sheet. In the output file, the 1st column is simply the image number for each image, the 2nd column is the 'sigNum' and the 3rd column is 'Skewness'. Save the Excel file.

3.5.2 Density Analysis: Image Processing

1. Select multiple (i.e., ca. 10) original files (.oib files), right click on the selected files, and choose '**Open With**', and select **Fiji** to open files.

2. A new '**Bio-Formats Import Options**' window will open. In the '**Bio-Formats Import Options**' window, at the '**Stack viewing**' panel, in '**View stack with:**', select '**Hyperstack**'. Remaining options (i.e., '**Dataset organization**', etc.) can be left at the default settings. From '**Color options**' panel, select '**Grayscale**'. From '**Split into separate windows**', check the box for '**Split channels**'. Select '**OK**' to complete format settings.

At this point, 2 windows will open, one that represents the confocal image, the other representing the brightfield image (Fig. 3a, b).

The remaining stack images from the experiment should be processed in the same fashion as above **steps 1–3**. As above, additional images (i.e., confocal and brightfield) will be created for each of the image stack .oib files. Repeat **steps 1–2** for each stack image. Each additional input stack image will yield a confocal and brightfield image.

3. Close all brightfield image windows (i.e., Fig. 3b). Leave the windows containing fluorescent actin filament images open (Fig. 3c).

The next step should be performed using the confocal microscopy-generated .oib images, processed as described above (i.e., those that are each contained within a separate window).

4. To apply the **Gaussian Blur** filter, choose 1 image, and from the Fiji 'Menu' bar select **Process ▶ Filters ▶ Gaussian Blur** (*see* **Note 8**).

5. In the '**Gaussian Blur**' dialog box, set '**Sigma (Radius)**' **1.0**, select '**OK**' (Fig. 3d).

6. A window '**Process Stack?**' will appear, select '**Yes**' to process all 25 images (25 series stacks).

7. Select the next image, click on it and repeat **step 4–6** until the remaining 9 images have been processed.

8. To apply the **HBP** filter, choose 1 image (.oib file generated from **steps 5–7**) and select **Process ▶ FFT ▶ Bandpass Filter** (*see* **Note 9**).

9. From the '**FFT Bandpass Filter**' window, select '**Filter large structures down to**' **40** pixels, '**Filter small structures up**
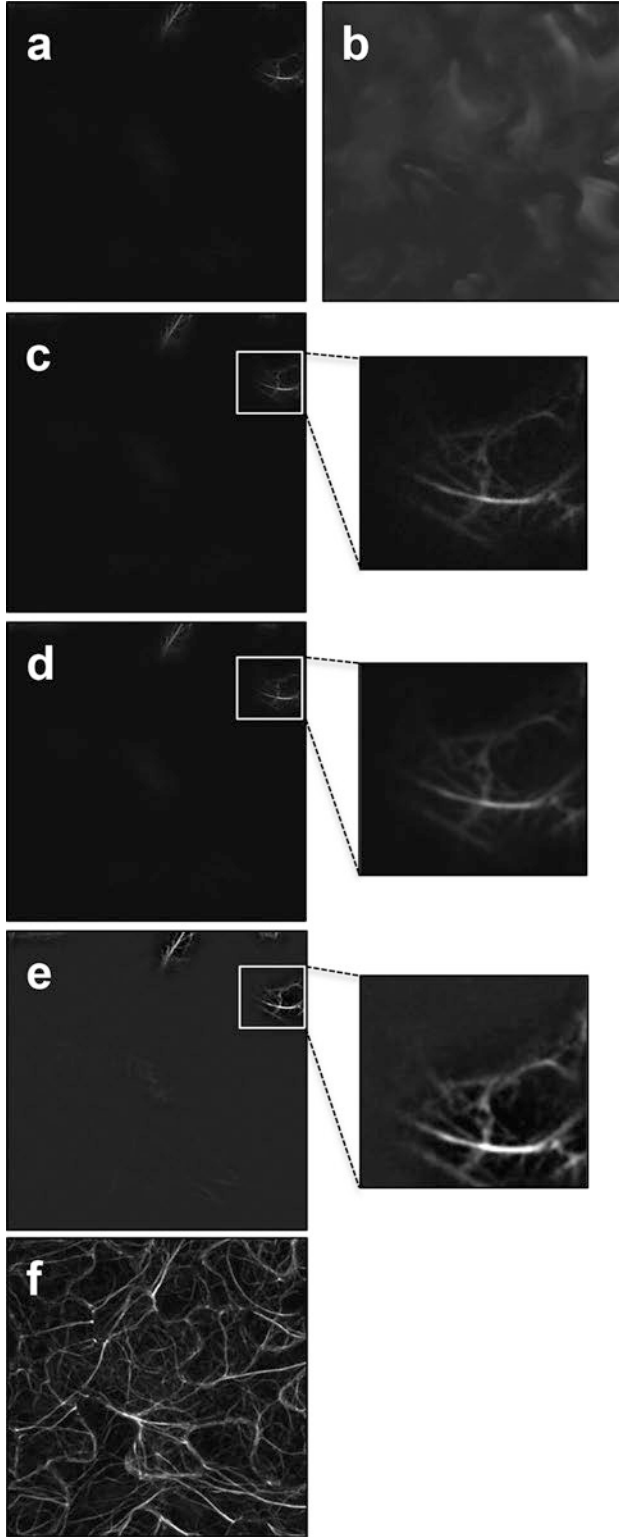
to' 0 pixels, '**Tolerance of direction**' to **0**%. Ensure that all boxes are unchecked, then select '**OK**'.

10. Repeat **step 9** for the remaining images.

11. To project serial stacks into 3D images: select 1 image processed as above (i.e., **step 10**). From the Fiji menu, select **Image ► Stacks ► Z Project**.

12. From the '**ZProjection**' window, set '**Start slice**' to **1**, '**Stop slice**' to **25**, '**Projection type**' to '**Max Intensity**', then select '**OK**'. Repeat for each image.

Completion of step 12 *will result in the generation of a new .oib file, representing the merged image with a maximum projection. The new file will be automatically named with the prefix 'MAX', preceding the original file name. At this point, the original .oib file can be closed, and <u>changes should not be saved</u>.*

13. Using the '**MAX**' image, at the Fiji menu, select **File ► Save As ► Tiff**. Create a 'New folder' and save '**MAX**' 3D images in this folder. ► Close windows.

14. Repeat **step 13** for the remaining '**MAX**' 3D images.

*Completion of this step will result in the generation of maximum project, 3D, image files, named '*xxxx.oib.tiff*'. The resultant TIFF files will be used for 'Density Analysis: Quantitative Evaluation', immediately below.*

Density Analysis: Quantitative Evaluation

1. From the Fiji menu, select **File ► Import ► Image Sequence**, and choose the new folder containing images (in **.oib.tiff** format) generated above (**step 15**) to be analyzed. Highlight the folder, and select '**Choose**'.

2. A new dialog window, '**Sequence Options**', will open. At this step, leave all settings at the default options, with the exception of '**Convert to 8-bit Grayscale**', which should be selected. Click '**OK**'.

Fig. 3 A sample of four images stacks analyzed for quantitative evaluation of the Density metric. (**a**, **b**) are confocal and bright field images, respectively, generated by the confocal laser scanning microscopy. The bright field image, which is also created during the Density analysis (Subheading 3.5.2) is shown, yet is not used for quantitative evaluation (Subheading 3.5.2, **step 3**). (**c**) The original, unprocessed, confocal image. (**d**) The same image as (**c**) following processing using the Gaussian Blur filter. (**e**) The same image as in (**d**) following processing with the high bandpass (HBP) filter. (**f**) The HBP filter processed stacks for each of the 25 collected images, merged, to yield a processed 3D image. This processed image is used as the input file for quantitative Density analysis

A new window will open that contains all of the processed images. The individual images can be viewed by scrolling the sliding tab at the bottom of the window, left-to-right.

3. For image analysis, begin at the 1st image (sliding tab to far left). From the Fiji menu, select **Image ▶ Adjust ▶ Threshold**. In 'Threshold' window, check the box for '**Dark Background**'. Select **'Set'**, which will open a new dialog window **'Set Threshold Levels'.** Set '**Lower Threshold Level**' to **25**, and the '**Upper Threshold Level**' to **255**. Click '**OK**'. In the '**Threshold**' dialog, click '**Apply**', a '**Convert Stack to Binary**' window will appear, check '**Black background (of binary masks)**', click '**OK**'. Leave the '**Threshold**' dialog window open.

4. From the Fiji menu, select **Plugin ▶ Macros ▶ Install ▶** locate the 'Density' script (.txt file), downloaded as described above. Once located, highlight the file, and select '**Open**'.

5. Return to the main Fiji menu and select **Plugin ▶ Macros ▶ Density**.

At this point, a new dialog window will open, 'Results', and the actin filament density analysis will initiate. The 'Area' will be calculated for each image processed, with the corresponding image number located to the immediate left of the 'Area'.

6. Copy these data from the dialog window and paste into Excel. Save the resultant Excel file.

3.5.3 Quantification and Presentation of Skewness and Density Parameters

For each cotyledon, five different areas of the epidermal pavement cells are imaged to ensure a non-biased selection for analysis. Additionally, for each technical repeat, at least 25 images of cotyledon epidermal cells per genotype with each treatment are collected. This results in a total of approximately 75 images per treatment (i.e., 3 biological repeats × 25 images per experiment). Once all images are collected and analyzed using the *Skewness* and *Density* parameters, mean values, standard errors, and the standard deviation is calculated using Microsoft Excel. A one-tailed Student's *t*-test should be employed to determine statistical significance. Data can be plotted using the mean values, with error bars indicating standard deviations (Fig. 4).

4   Notes

1. Most potting soil mixtures designed for Arabidopsis growth work well for this procedure. We typically use Redi-earth (Hummert International, Earth City, MO, USA), which we have observed maintains soil moisture and does require frequent watering.
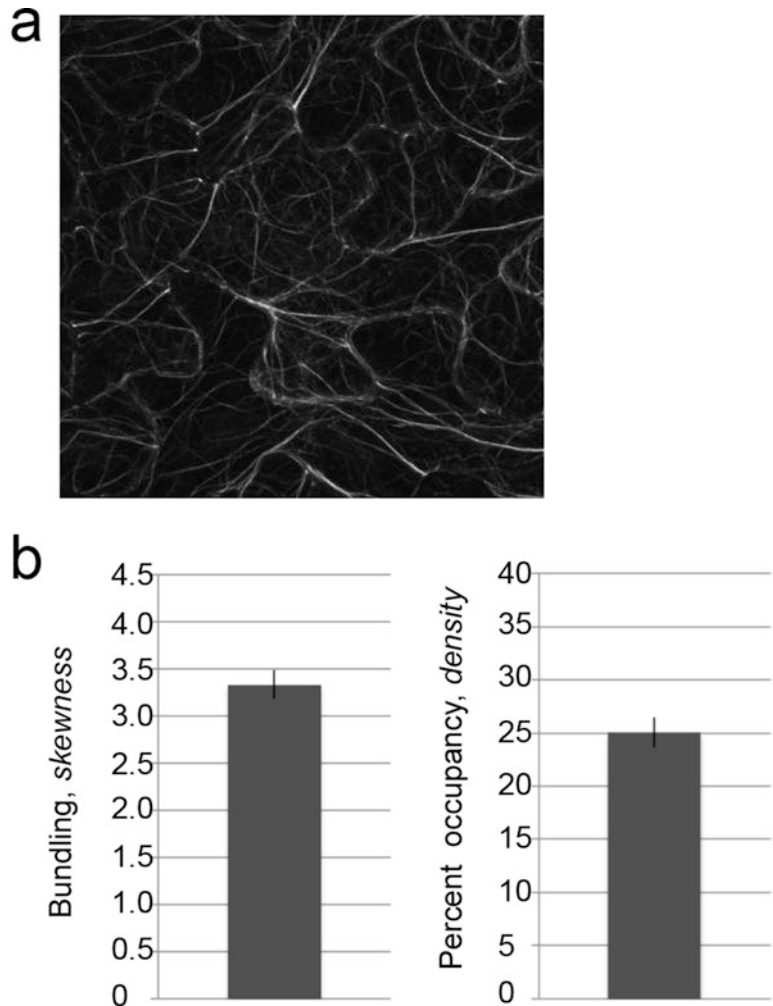
Fig. 4 Quantitative analysis of skewness and density metrics following pathogen elicitation of 12–14-day-old Arabidopsis seedlings. (**a**) Representative picture of finalized image. (**b**) Actin skewness and density are analyzed quantitatively. The data presented in the left graft (Bundling, *skewness*) represents the raw output values generated in Subheading 3.5.1. For presentation of the data shown in the graph on the right (% occupancy, *density*), the final output values (Subheading 3.5.2) are calculated whereby "% occupancy" is represented as: [100 × (Area ÷ 640,000)]. This calculation was originally described by Higaki and colleagues [8]

2. There are several companies that synthesize high quality peptides. In our experience, we have found that EZ-Biolabs (Carmel, Indiana, USA) provides high-quality peptides at a level of synthesis sufficient to last several years.

3. To ensure minimal physical injury to plant seedlings, as well as to keep the plants and soil undisturbed during the dip-inoculation procedure, we cover the soil with a fiberglass

mesh insect screen (i.e., BetterVue; Phifer Inc., Tuscaloosa, Alabama, USA), held in place with a rubber band. The screen should be cut to approximately 1-in. larger (on each side) than the dimensions of the pot.

4. We have observed a density-dependent (i.e., dose response) change in the Arabidopsis actin cytoskeleton following pathogen inoculation. To compensate for the differential growth of bacterial strains which may show significant differences in growth at 24 hpi, we recommend evaluating, side-by-side, the *in planta* growth of each strain to be used, and if direct comparisons are to be made between strains that show differential growth at 24 hpi, to make adjustments in the initial inoculum concentration such that each strain reaches a similar CFU at the desired time of imaging [6]. Additionally, the incubation time may vary depending on whether or not the *Pst* DC3000 is heterologously expressing a T3E that elicits the hypersensitive cell death response. If this is the case, a shorter incubation period (e.g., 16 hpi) may be required to image samples before the onset of cell death.

5. In our experience, we have observed silencing of the GFP-fABD2 transgene after approximately 6–8 generations of self-propagation. To circumvent problems with silencing, we typically generate multiple lines, collect an abundance of seed at each generation, and initially characterize multiple lines of each. Through this process, one can effective prolong the life of a given line, ensuring consistency in the interpretation of independent experiments.

6. Always use consistent settings for exposure time and gain for actin observation.

7. The best results are obtained when you select a relatively flat area of the cotyledon for imaging. This will ensure that the plane of vision is in focus. Also, avoid stomatal guard cells when imaging. The guard cells contribute an abundance of background fluorescence to the sample, and thus, can skew the data in favor of increased signal intensity.

8. Gaussian blur, also referred to Gaussian smoothing, is the result of blurring an image to effectively reduce image noise and detail, enabling the user to evaluate the image as a function of the individual pixels within the image. This "low pass" filtering technique for the analysis of high-resolution images results in the removal of both high and low spatial frequencies, resulting in an image that retains the middle range of the image qualities, enhances the image signals (i.e., pixels) at the edge, while reducing image noise [8].

9. The Bandpass filter is applied to minimize background autofluorescence. This is particularly important when visualizing

plant cells using laser scanning confocal microscopy, as green tissues typically exhibit high levels of chloroplast-derived autofluorescence.

Acknowledgments

References

1. Day B, Henty JL, Porter KJ, Staiger CJ (2011) The pathogen-actin connection: a platform for defense signaling in plants. Annu Rev Phytopathol 49:483–506

2. Henty-Ridilla JL, Shimono M, Li J, Chang JH, Day B, Staiger CJ (2013) The plant actin cytoskeleton responds to signals from microbe-associated molecular patterns. PLoS Pathog 9:e1003290

3. Porter K, Shimono M, Tian M, Day B (2012) Arabidopsis actin-depolymerizing factor-4 links pathogen perception, defense activation and transcription to cytoskeletal dynamics. PLoS Pathog 8:e1003006

4. Tian M, Chaudhry F, Ruzicka DR, Meagher RB, Staiger CJ, Day B (2009) Arabidopsis actin-depolymerizing factor AtADF4 mediates defense signal transduction triggered by the *Pseudomonas syringae* effector AvrPphB. Plant Physiol 150:815–824

5. Shimono M, Higaki T, Kaku H, Shibuya N, Hasezawa S, Day B (2016) Quantitative evaluation of stomatal cytoskeletal patterns during the activation of immune signaling in *Arabidopsis thaliana*. PLoS One 11:e0159291

6. Shimono M, Lu YJ, Porter K, Kvitko BH, Henty-Ridilla J, Creason A, He SY, Chang JH, Staiger CJ, Day B (2016) The *Pseudomonas syringae* type III effector HopG1 induces actin remodeling to promote symptom development and susceptibility during Infection. Plant Physiol 171:2239–2255

7. Dong B, Yang X, Zhu S, Bassham DC, Fang N (2015) Stochastic optical reconstruction microscopy imaging of microtubule arrays in intact *Arabidopsis thaliana* seedling roots. Sci Rep 5:15694

8. Higaki T, Kutsuna N, Sano T, Kondo N, Hasezawa S (2010) Quantification and cluster analysis of actin cytoskeletal structures in plant cells: role of actin bundling in stomatal movement during diurnal cycles in Arabidopsis guard cells. Plant J 61:156–165

9. Shaw SL, Ehrhardt DW (2013) Smaller, faster, brighter: advances in optical imaging of living plant cells. Annu Rev Plant Biol 64:351–375

10. Dyachok J, Paez-Garcia A, Yoo CM, Palanichelvam K, Blancaflor EB (2016) Fluorescence imaging of the cytoskeleton in plant roots. Methods Mol Biol 1365: 139–153

11. Daniels MJ, Barber CE, Turner PC, Sawczyc MK, Byrde RJ, Fielding AH (1984) Cloning of genes involved in pathogenicity of *Xanthomonas campestris* pv. *campestris* using the broad host range cosmid pLAFR1. EMBO J 3:3323–3328

12. Sheahan MB, Staiger CJ, Rose RJ, McCurdy DW (2004) A green fluorescent protein fusion to actin-binding domain 2 of Arabidopsis fimbrin highlights new features of a dynamic actin cytoskeleton in live plant cells. Plant Physiol 136:3968–3978

13. Zipfel C (2014) Plant pattern-recognition receptors. Trends Immunol 35:345–351

14. Kaku H, Nishizawa Y, Ishii-Minami N, Akimoto-Tomiyama C, Dohmae N, Takio K, Minami E, Shibuya N (2006) Plant cells recognize chitin fragments for defense signaling through a plasma membrane receptor. Proc Natl Acad Sci U S A 103:11086–11091

15. Felix G, Duran JD, Volko S, Boller T (1999) Plants have a sensitive perception system for the most conserved domain of bacterial flagellin. Plant J 18:265–276

16. Kunze G, Zipfel C, Robatzek S, Niehaus K, Boller T, Felix G (2004) The N terminus of bacterial elongation factor Tu elicits innate immunity in Arabidopsis plants. Plant Cell 16:3496–3507